Preparation and Curing Kinetics of Bisphenol A Type Novolac Epoxy Resins

Yanfang Liu,[1,2] Chen Zhang,[1] Zhongjie Du,[1] Hangquan Li[1]

[1]*School of Materials Science and Engineering, Beijing University of Chemical Technology, Beijing 100029, China*
[2]*College of Chemistry and Environmental Science, Hebei University, Baoding 071002, China*

Received 22 October 2004; accepted 11 April 2005
DOI 10.1002/app.22735
Published online in Wiley InterScience (www.interscience.wiley.com).

ABSTRACT: A bisphenol A type novolac resin (Bis-ANR) was synthesized from bisphenol A and formaldehyde; the resulting novolac was epoxidized to generate a bisphenol A type novolac epoxy resin (Bis-ANER). The chemical structures of Bis-ANR and Bis-ANER were confirmed by ^{1}H-NMR spectroscopy and IR spectroscopy; the molecular weights and molecular weight distributions were determined by gel permeation chromatography. In addition, the curing process of Bis-ANER with 4,4′-diaminodiphenyl sulfone was studied in both dynamic and isothermal modes with differential scanning calorimetry. The dynamic curing kinetic analysis was evaluated with both the Kissinger and Flynn–Wall–Ozawa methods, and the curing activation energy values were obtained. The isothermal curing reaction exhibited autocatalytic behavior, and the curing kinetics were described with the Kamal kinetics model, which accounted for both the autocatalytic and diffusion-control effects. © 2005 Wiley Periodicals, Inc. J Appl Polym Sci 99: 858–868, 2006

Key words: composites; curing of polymers; kinetics (polym.); matrix; resins

INTRODUCTION

Epoxy resins possess excellent mechanical properties, water resistance, chemical resistance, heat resistance, electrical properties, and so on. They are widely used as encapsulating and packing materials in the electronics industry and as the matrix of high-performance, fiber-reinforced composites in the aerospace and automotive industries. The most commonly used epoxy resins are those obtained via the reaction of epichlorohydrin (ECH) with bisphenol A (BPA). However, in the high-technology area, high-performance epoxy resins with high thermal and moisture resistance and low thermal expansion coefficients have attracted increasing attention.

To improve the thermal and mechanical properties of epoxy resins, the modification of the molecular backbone and/or an increase in the number of epoxide group functionalities are the generally employed methods.[1,2] Novolac epoxy resins, being multifunctional, can produce a denser crosslinked network compared to common epoxy resins.[2] They are characterized by an outstanding combination of both mechanical and chemical properties in terms of high modulus, thermal stability, and solvent resistance and, therefore, find wide applications as sealing media for semiconductor devices.

The traditional method for the preparation of a novolac resin was a condensation polymerization between formaldehyde and phenol in the presence of an acid or an alkali.[3,4] Generally, hydrochloric acid, sulfuric acid, *p*-toluene sulfuric acid, or oxalic acid was used as a catalyst.[5,6] Determined by the mechanism, with an acid catalyst, a linear thermoplastic bisphenol A type novolac resin (Bis-ANR) could be obtained, which was subsequently reacted with epihalohydrin in an alkali media to generate a bisphenol A type novolac epoxy resin (Bis-ANER).

Bis-ANER is a multifunctional epoxy resin and its molecular backbone consists mainly of aromatic rings; as a result, it may have excellent mechanical and thermal performance after proper curing. The performance of the cured resin depends on the network structure, which in turn, depends sensitively on the curing condition. Multiple chemical reactions between Bis-ANER and curing reagents give rise to a complex kinetic behavior, and the physical state of the resin changes with the crosslinking developed. A comprehensive understanding of the mechanism and kinetics of curing can lead to an optimal curing process.

Correspondence to: H. Li (hli45@yahoo.com.cn).

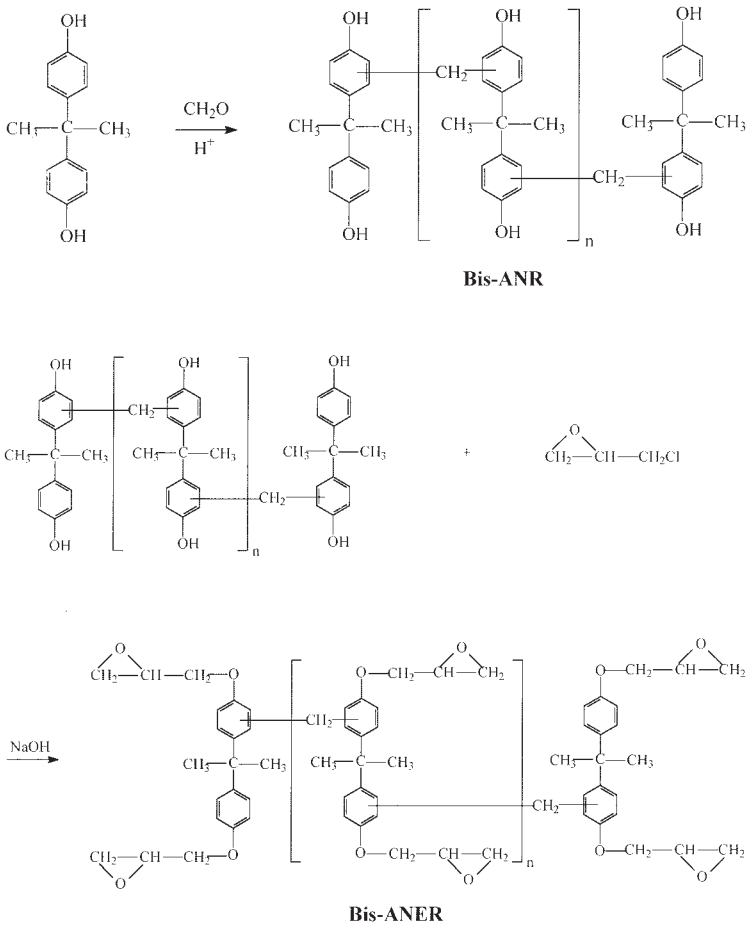

Scheme 1 Syntheses of Bis-ANR and Bis-ANER.

In this study, Bis-ANR and Bis-ANER were prepared, and the curing kinetics of Bis-ANER with 4,4′-diaminodiphenyl sulfone (DDS) were evaluated with both dynamic and isothermal differential scanning calorimetry (DSC).

EXPERIMENTAL

Materials

BPA (CP), formaldehyde (37% aqueous), and *n*-butanol (AR) were obtained from Beijing Chemical Co. (China). ECH, oxalic acid, sodium hydroxide, and benzene were obtained from Tianjin Chemical Co. (China). Tetrabutylammonium bromide and DDS were obtained from Shanghai Chemical Co. (China). All solvents were used as received without further purification.

Synthesis of Bis-ANR[7–9]

To a 100-mL, three-necked, round-bottom flask equipped with a mechanical stirrer and a reflux condenser, BPA (22.8 g, 0.1 mol) and *n*-butanol (25 mL) as a solvent were added. The mixture was first heated to 80°C with stirring until the BPA was completely dissolved; the solution was allowed to cool to room temperature and then 37 wt % formalin (8.1 g, 0.1 mol) and oxalic acid (0.26 g, 0.002 mol) as catalyst were added. Subsequently, the flask was kept between 95 and 100°C to carry out the condensation for 6 h. The water generated and the *n*-butanol were distilled off at atmospheric pressure first and under reduced pressure with the temperature kept below 150°C. The product was washed several times with boiling water to remove the impurities and unreacted BPA. Finally, water was removed under a reduced pressure, and a light yellow transparent solid Bis-ANR product was obtained. The synthetic scheme is shown in Scheme 1.

Synthesis of Bis-ANER[8–10]

To a 100-mL, three-necked, round-bottom flask equipped with a mechanical stirrer and a reflux condenser, 6.5 g of the previously synthesized Bis-ANR,

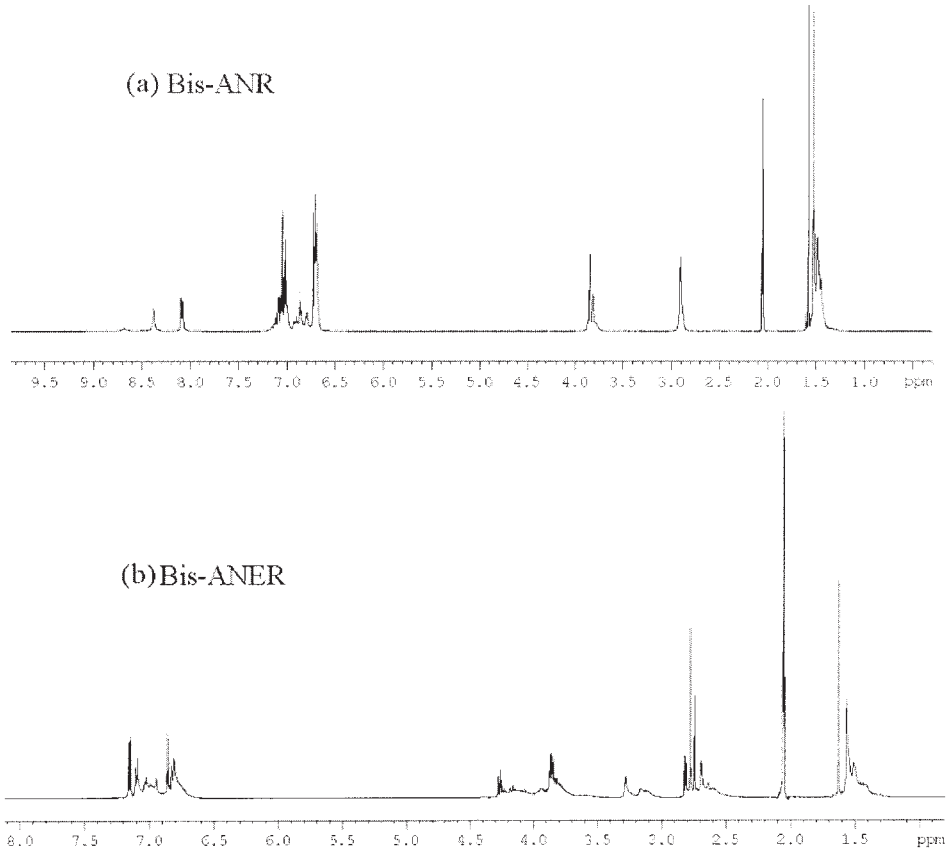

Figure 1 ^{1}H-NMR spectra of (a) Bis-ANR and (b) Bis-ANER in acetone–d_6.

30 mL of ECH, and 0.15 g of tetrabutylammonium bromide as a catalyst were added. The mixture was first allowed to react with stirring at about 100°C for 3 h. Thereafter, the resulting mixture was cooled to 55–60°C; this was followed by the addition of 25 mL of 10 wt % NaOH (aqueous) dropwise through a dropping funnel with stirring over 1.5 h. After the addition of sodium hydroxide, the reaction was continued for additional 1 h at 65–70°C. Subsequently, the system was washed with water several times to remove the formed salts. The excess ECH was evaporated from the organic phase under reduced pressure, and the remaining system was dissolved in benzene and extracted with water several times. Finally, the organic phase was distilled to remove benzene and water, and a light yellow transparent solid Bis-ANER product was obtained. The synthetic route is shown in Scheme 1.

Characterization

With deuterated acetone solvent, ^{1}H-NMR spectra were recorded on a Bruker AV-600 NMR spectrometer, and tetramethylsilane was used as the internal standard. The operating parameters for ^{1}H-NMR were as follows: sweep width = 600 MHz, pulse width = 5.80 μs, and number of scans = 16.

Fourier transform infrared spectra were obtained on a Nicolet Nexus 670 spectrometer in the range 4000–400 cm^{-1}. The resin was first mixed with potassium bromide, and the mixture was pressed into a plate, which was used for scanning.

The molecular weight and the molecular weight distribution values of the resins were determined with a Waters gel permeation chromatograph equipped with a 515 HPLC pump, a 717 auto sample injector, Styragel (HT3_HT5_HT6E) columns, a 2410 refractive index detector, and a 996 photodiode array detector (at 254 nm). The gel permeation chromatography (GPC) measurements were performed at a column temperature of 30°C with tetrahydrofuran as the mobile phase and at a flow rate of 1.0 mL/min. The concentration of the samples was 2 mg/mL in tetrahydrofuran, and the injecting amount for measurement was 50 μL. The molecular weights of the samples were calibrated with monodisperse polystyrene standards.

The curing behavior of Bis-ANER was studied with a Shimadzu DSC-41 differential scanning calorimeter operating in a nitrogen atmosphere. The

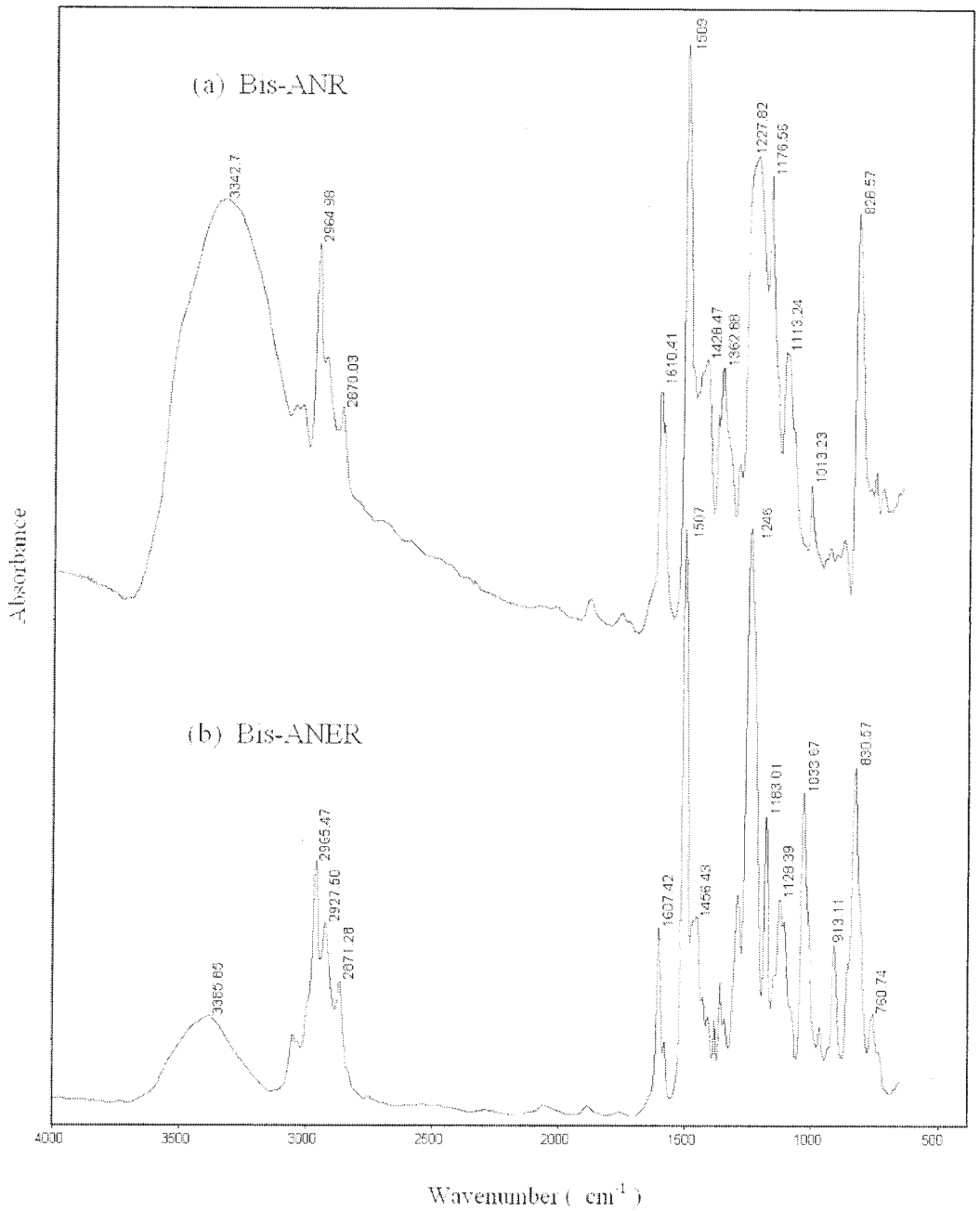

Figure 2 Fourier transform infrared spectra of (a) Bis-ANR and (b) Bis-ANER.

DSC instrument was calibrated by an indium standard. α-Al_2O_3 was used as the reference material. The Bis-ANER/DDS sample was prepared with a stoichiometric ratio of one epoxy group versus one amine hydrogen. The amount of sample used was about 10 mg. In the dynamic analysis, the samples were scanned at five heating rates: 2.5, 5, 7.5, 10, and 12.5°C/min. Isothermal analysis was performed at four temperatures: 178, 188, 198, and 208°C. Before loading the sample, the furnace was first heated to a desired temperature and kept for a certain period of time. When the system reached an equilibrium state, the sample cell was quickly set on the calorimetric detector plate. The reaction was considered complete when the rate curve leveled off to a baseline.

In addition, the softening temperatures (T_s's) of Bis-ANR and Bis-ANER were measured with DSC. According to the operation procedure mentioned previously, samples with the same weight (10 mg) were scanned in the DSC-41 at 10°C/min, and T_s was taken as the midpoint of the heat capacity change.

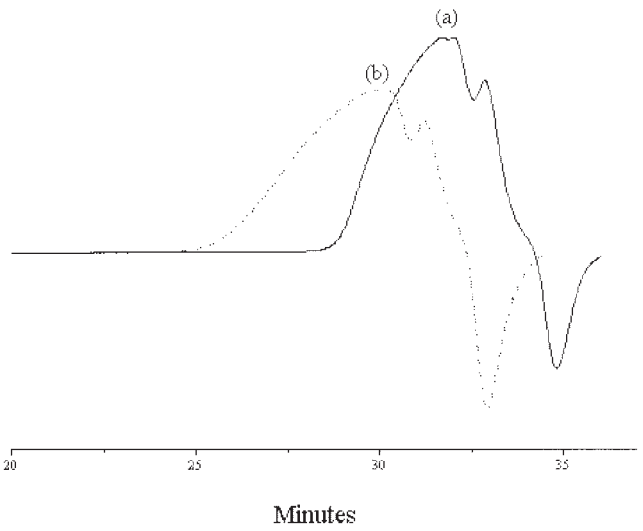

Figure 3 GPC curves of (a) Bis-ANR and (b) Bis-ANER.

RESULTS AND DISCUSSION

Synthesis and characterization

Bis-ANR was obtained via the reaction of BPA with formaldehyde with oxalic acid as a catalyst, and the preparation of Bis-ANER involved the reaction of Bis-ANR with a halohydrin in the presence of an alkali metal hydroxide, as shown in Scheme 1. The chemical structures of Bis-ANR and Bis-ANER were confirmed by ^{1}H-NMR and IR spectroscopy.

The ^{1}H-NMR spectrum of Bis-ANR in acetone–d_6 is shown in Figure 1(a). Multiplet peaks at 1.491–1.585, 3.817–3.846, 6.692–7.058, and 8.081–8.684 ppm were assigned to methyl, methylene bridges, aromatic, and hydroxyl protons, respectively. Methylene bridges are the characteristic structure of Bis-ANR. In addition, two multiplet peaks corresponding to the aromatic protons on the phenol ring at 6.692–6.728 ppm (ortho to the phenolic hydroxyl group) and 7.016–7.058 ppm (meta to the phenolic hydroxyl group) were observed symmetrically about a central point; this was because BPA is a parasubstituted aromatic compound in which two substituents differ from each other in electronic effects. However, compared with the ^{1}H-NMR spectrum of BPA, the symmetrical pattern became complex, and some split peaks appeared between 6.728 and 7.016 ppm, which were assigned to the effect of the methylene bridges bonding to the aromatic rings. In fact, the eight active positions on BPA for the methylene bridges to bond to the aromatic rings could be categorized as two kinds, ortho and meta positions. The two kinds of positions appeared to possess the same bonding chance to the methylene bridges, which was indicated by the ratio of the peak areas for the two kinds of aromatic protons. Moreover, the ratio of area integrations for the peaks (Ph—CH_2—Ph/aromatic protons/Ph—C—CH_3) in Figure 1(a) was consistent with the proposed statistical structure of Bis-ANR shown in Scheme 1 for $n = 1$. In practice, several synthesized products were determined by ^{1}H-NMR spectroscopy in this study, and an average n of 2 was obtained for certain resins.

In the ^{1}H-NMR spectrum of Bis-ANER in acetone–d_6 [Fig. 1 (b)], the same signal pattern as for Bis-ANR was observed, except for the signals corresponding to the glycidyl group. Assignments of the chemical shifts (ppm) were as follows: 1.627 (singlet, methyl protons), 2.695–2.827 (multiplet, protons of methylene in the oxirane ring), around 3.282 (multiplet, protons of methine in the oxirane ring), 4.270–4.288 (multiplet, protons of methylene connected the phenoxy and the oxirane ring), 3.846–3.875 (multiplet, methylene bridges protons), and 6.811–6.865 and 7.093–7.161 (multiplet, aromatic protons on phenoxy ring). These results strongly supported the structure of Bis-ANER shown in Scheme 1.

Figure 2 presents the IR spectra of Bis-ANR and Bis-ANER. For the spectrum of Bis-ANR, the absorption at 3342 cm^{-1} was assigned to the stretching vibrations of the phenolic hydroxyl group. For the spectrum of Bis-ANER, the absorption at 913 cm^{-1} was assigned to the oxirane rings.

Figure 3 shows the gel permeation chromatograms of Bis-ANR and Bis-ANER. The number-average molecular weight (M_n), weight-average molecular weight (M_w), and polydispersity index (M_w/M_n) values calculated from the GPC results are presented in Table I. The GPC traces showed a clear bimodal distribution, this indicated that the products mainly consisted of

TABLE I
Molecular Weight and Molecular Weight Dispersion Values of Bis-ANR and Bis-ANER Determined with GPC

Resin	M_n	M_w	M_z	M_{z+1}	M_p	$\frac{M_w}{M_n}$
Bis-ANR	1343	1908	2673	3,448	740	1.42
Bis-ANER	1422	3174	7658	13,336	1145	2.23

M_z, z-average molecular weight; M_p, molecular weight at GPC peak.

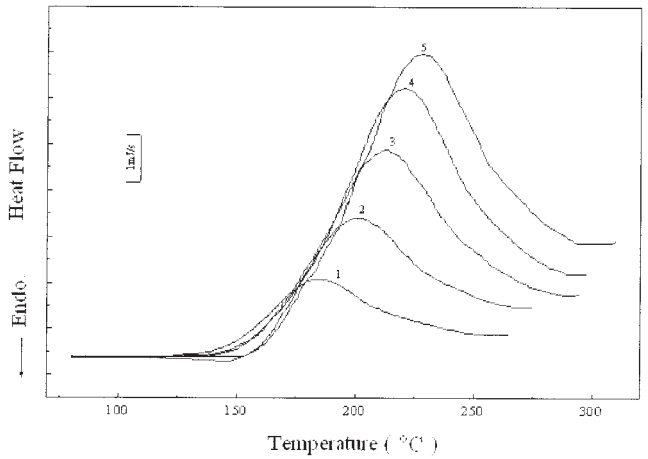

Figure 4 Dynamic curing DSC curves of the Bis-ANER/DDS system: (1) 2.5°C/min; (2) 5°C/min; (3) 7.5°C/min; (4) 10°C/min; (5) 12.5°C/min.

trimers and dimers, and the n numbers in most molecules were higher than unity.

The epoxy equivalent weight of the synthesized Bis-ANER was 213 g/equiv, which was determined by the hydrochloric acid–acetone method. The T_s values of Bis-ANR and Bis-ANER determined with DSC were 85 and 36°C, respectively.

Curing reaction of Bis-ANER and DDS

Bis-ANER, when cured with DDS, can be converted into a highly crosslinked three-dimensional network. The reaction during the curing of Bis-ANER with DDS was between the epoxy groups and the active hydrogens on the amine. The reaction steps included the addition of a primary amine active hydrogen to an epoxy group, followed by the addition of the resulting secondary amine hydrogen to another epoxy group. The curing behavior of an epoxy resin depends on both temperature and time, which affect not only the physical properties of the resulted material but also the curing kinetics.

The curing reaction kinetics of the thermosetting resins were characterized with DSC with both dynamic and isothermal modes. In the dynamic mode, the curing reaction kinetic parameters were evaluated with a multiple-heating-rate method by the determination of the exothermic peak temperatures (T_p's) at several heating rates. In practice, two convenient multiple-heating-rate methods are generally used. One is the maximum reaction rate ($d\alpha/dt$) method proposed by Kissinger,[11] which is based on the fact that T_p varies with the heating rates. The other is the isoconversion method proposed by Flynn and Wall[12] and Ozawa,[13] which is based on the fact that isoconversion can be reached at different temperatures with various heating rates. The two methods can be used in a variety of curing reaction systems without consideration of the reaction mechanism.

Kissinger's technique assumes that the maximum $d\alpha/dt$ occurs at peak temperatures, where $d^2\alpha/dt^2 = 0$, can be expressed as

$$\ln\left(\frac{\beta}{T_p^2}\right) = \ln\left(\frac{AR}{E}\right) - \frac{E}{RT_p} \quad (1)$$

where β is the linear heating rate, A is the preexponential factor, E is the activation energy, and R is the universal gas constant. Therefore, a plot of $\ln(\beta/T_p^2)$ versus $1/T_p$ gives the values of E and A.

The Flynn–Wall–Ozawa method assumes that the degree of conversation at peak temperatures for different heating rates is constant. It can be expressed as

$$\log \beta = -\frac{0.4567E}{RT} + C \quad (2)$$

where C is a constant, T is the isoconversion temperature, and the other parameters are the same as described previously. E can be obtained from the slope of the plot of $\log \beta$ versus $1/T_p$.

The dynamic curing DSC curves of Bis-ANER with DDS system are shown in Figure 4. The exothermic reaction proceeded in a wide temperature range, and both the onset and the maximum rate temperatures of the curing reaction varied with the heating rate. All of the T_p values of the DSC curves at different heating rates are listed in Table II. The curing kinetic parameters determined by the Kissinger and Flynn–Wall–Ozawa methods are also summarized in Table II. If the results obtained by the two methods are compared, one can see that the E value obtained by the Flynn–Wall–Ozawa method was slightly higher than that obtained by the Kissinger method.

TABLE II
T_p (°C) and Kinetic Parameter Values Obtained from the Dynamic DSC Scan

Heating rate (°C/min)					Kissinger		Flynn–Wall–Ozawa
2.5	5	7.5	10	12.5	E (kJ/mol)	A (s^{-1})	E (kJ/mol)
184.7	200.8	212.8	220.4	228.3	62.7	1310	67.1

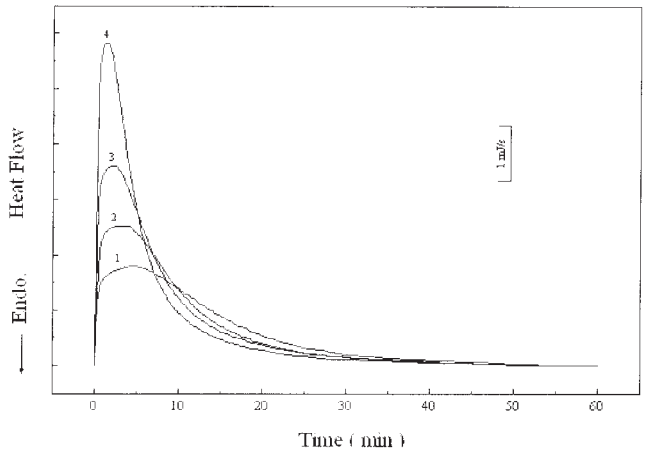

Figure 5 Isothermal curing DSC curves of the Bis-ANER/DDS system: (1) 178°C/min; (2) 188°C/min; (3) 198°C/min; (4) 208°C/min.

In isothermal DSC mode, the curing reaction kinetics can be characterized by the measurement of the heat generated during the curing reaction as a function of temperature and time. In general, the heat evolution recorded by DSC was assumed to be proportional to the extent of the consumption of the reactive groups. According to this assumption, the extent of the reaction (α) and $d\alpha/dt$ during the curing process can be described as follows:

$$\alpha = \frac{\Delta H_t}{\Delta H_0} \tag{3}$$

$$\frac{d\alpha}{dt} = \frac{1}{\Delta H_0} \times \frac{dH}{dt} \tag{4}$$

where ΔH_t is the reaction heat within time t, dH/dt is the flow rate of heat, and ΔH_0 is the total reaction heat, which is the maximum heat value determined among all of the isothermal and dynamic curing reactions.

Several curing temperatures were chosen as the isothermal curing reaction temperatures of the Bis-ANER/DDS system. Figure 5 shows the isothermal curing DSC curves at different temperatures. It was evident that the heat flow rate was a function of the curing temperature and time. According to eqs. (3) and (4), α and $d\alpha/dt$ were calculated, and the plots of α versus t, $d\alpha/dt$ versus α at different temperatures are shown in Figures 6 and 7, respectively.

Figure 6 shows that α of the Bis-ANER/DDS system was affected by both curing temperature and time. At a given curing time, the higher the curing temperature was, the higher α was. In addition, at a given temperature, α increased rapidly at the initial reaction stage, then increased slowly to 0.6–0.8, and finally leveled off at a certain value. This was attributed to the sequential reactions of the chain extending, branching, and crosslinking of Bis-ANER/DDS during the curing process, which reduced the mobility of the reacting molecules and slowed down $d\alpha/dt$. According to the chemical kinetics and diffusion control theories, the curing reaction process can be divided into two stages: the chemical kinetics controlling stage and the diffusion controlling stage. With rising curing temperature,

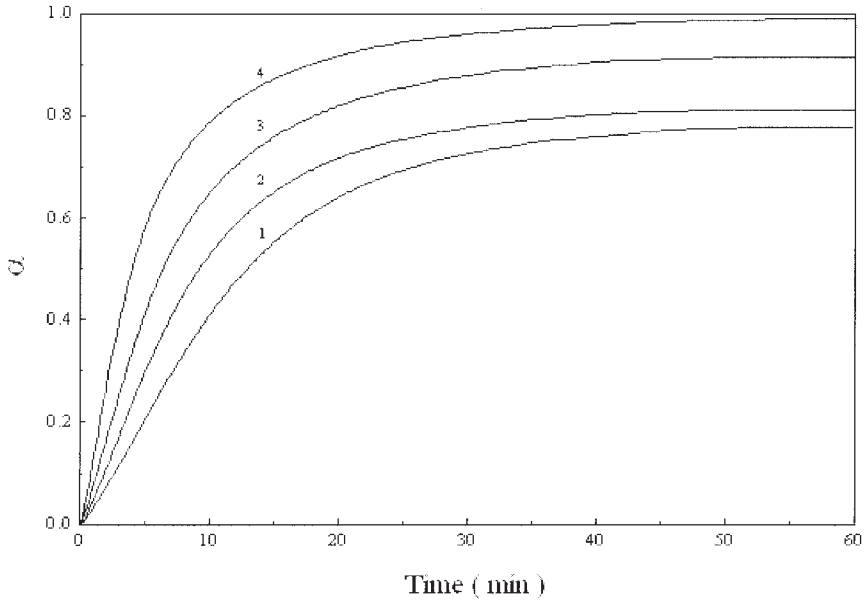

Figure 6 Plots of the conversion α versus t for the Bis-ANER/DDS system at different temperatures: (1) 178°C/min; (2) 188°C/min; (3) 198°C/min;(4) 208°C/min.

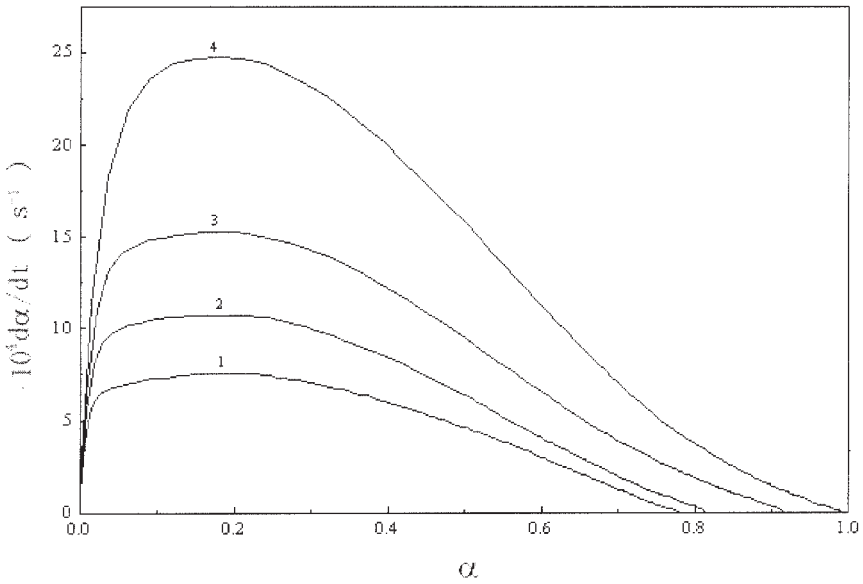

Figure 7 Plots of the curing $d\alpha/dt$ versus conversion α for Bis-ANER/DDS system at different temperatures: (1) 178°C/min; (2) 188°C/min; (3) 198°C/min; (4) 208°C/min.

the onset of diffusion controlling appeared at a point with a higher α value.

Figure 7 shows that $d\alpha/dt$ varied with the curing temperature and conversion. At a given temperature, $d\alpha/dt$ was observed to increase initially with conversion; it attained a maximum at about $\alpha = 0.2$ and subsequently and gradually slowed down until it finally reached zero at a certain degree of conversion. In addition, at a given conversion, the higher the isothermal temperature was, the higher $d\alpha/dt$ was. Moreover, a higher final conversion was obtained at a higher isothermal temperature.

Phenomenologically, the nth-order kinetics and autocatalytic kinetics are the two typical reaction mechanisms that describe the thermoset curing reaction. They can be expressed as nth-order kinetics

$$\frac{d\alpha}{dt} = k(T)(1 - \alpha)^n \tag{5}$$

and autocatalytic kinetics[14,15]

$$\frac{d\alpha}{dt} = (k_1 + k_2\alpha^m)(1 - \alpha)^n \tag{6}$$

where $k(T)$ is the rate constant at temperature T, m and n are the reaction orders, and k_1 and k_2 are the reaction rate constants with two different activation energies and preexponential factors. The two models are suitable for different characteristics. Systems obeying nth-order kinetics have a clear $d\alpha/dt$ maximum at $t = 0$, whereas systems obeying autocatalytic kinetics exhibits a maximum value at some intermediate conversion. As shown in Figure 7, the curing kinetic reaction mechanisms of Bis-ANER/DDS system followed the autocatalytic reaction; for this reason, eq. (6) was used to obtain the kinetic parameters.

k_1 in eq. (6) was calculated with the initial $d\alpha/dt$ at $t = 0$ from the intercept of the isothermal curve,[16,17] and eq. (6) could be simplified to

$$\left.\frac{d\alpha}{dt}\right|_{t=0} = k_1 \tag{7}$$

Other parameters in eq. (6) were obtained with a nonlinear regression method from the experimental data,[18,19] and the values of m, n, k_1, and k_2 for each curing temperature are shown in Table III. k_1 and k_2 increased with increasing curing temperature. The E values corresponding to k_1 and k_2 were 66.7 and 67.9 kJ/mol, respectively. These results show that the isothermal curing E values were close to that of the dynamic curing.

TABLE III
Isothermal Curing Parameters

Temperature (°C)	k_1 (10^{-3} s^{-1})	k_2 (10^{-3} s^{-1})	m	n
178	0.52	2.47	0.80	2.06
188	0.81	4.21	0.96	2.42
198	1.19	5.90	0.93	2.18
208	1.58	7.71	0.76	1.96

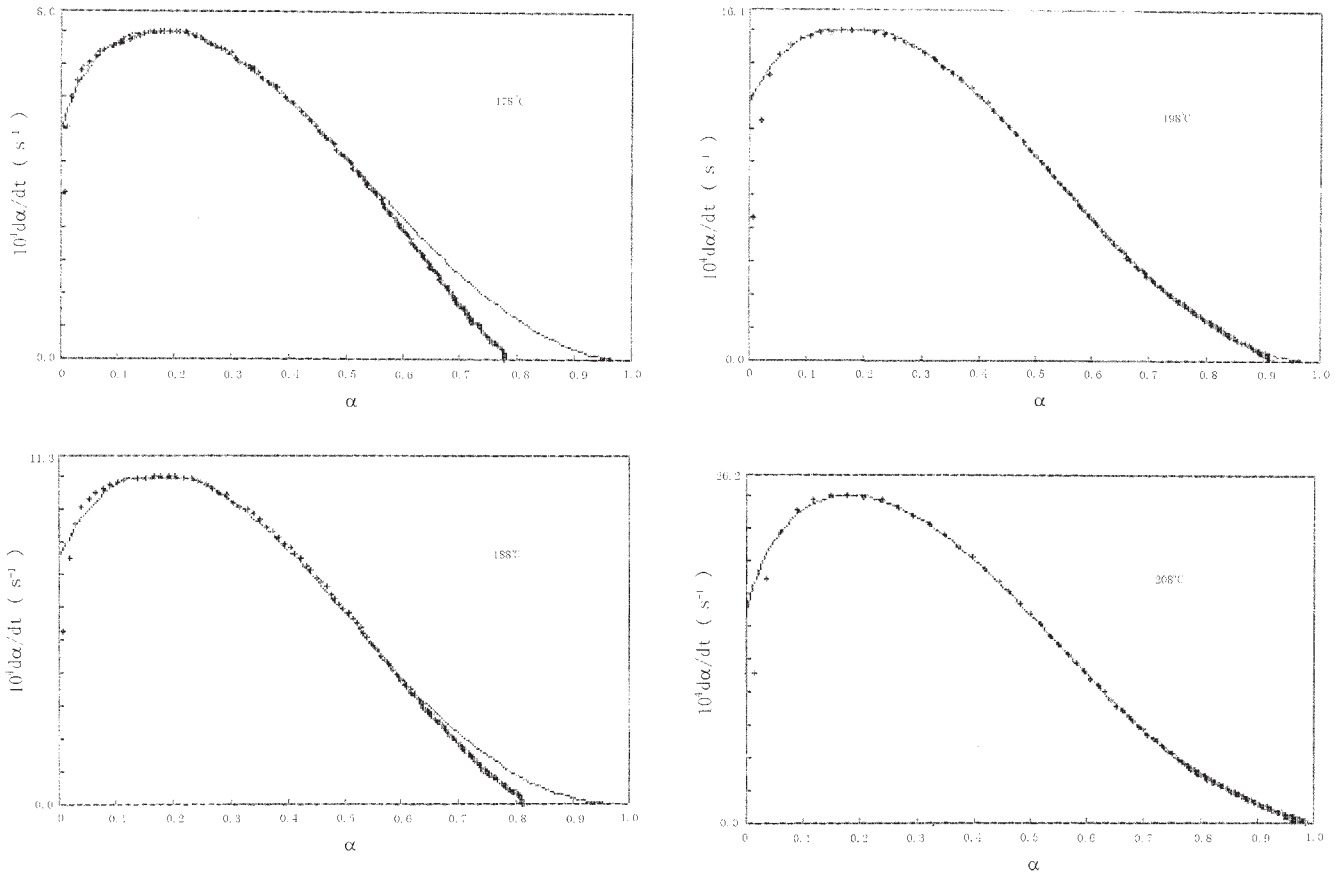

Figure 8 Comparison of (+) the experimental data with (· · ·) the kinetic model results for the Bis-ANER/DDS system at different temperatures.

Figure 8 compares the experimental data with those calculated with the Kamal equation for the curing of the Bis-ANER/DDS system. The model curves of $d\alpha/dt$ versus α matched the experimental data quite well in the whole curing reaction process at high temperatures, whereas deviations were observed in the later stage at low temperatures, which were attributed to the effect of diffusion. For this reason, we concluded that the curing $d\alpha/dt$ was affected by both chemical kinetics and diffusion, and the effects varied in different reaction stages and at different temperatures. At low curing temperatures, the effect of the diffusion on the later stage of the curing reaction was apparent. With increasing curing temperature, the fraction of the autocatalytic effect increased and that of the diffusion effect decreased, which diminished at 208°C. This indicated that the thermal energy could provide sufficient molecular mobility to recommence the curing process.[20] Therefore, in the Bis-ANER/DDS curing system, the higher the curing temperature was, the lower the effect of the diffusion was. Chemical kinetics dominated the whole curing reaction process at 208°C.

To characterize the diffusion control behavior at lower temperatures, a diffusion factor [$f(\alpha)$] could be defined as follows:[21]

$$f(\alpha) = \frac{k_e}{k_c} = \frac{1}{1 + \exp[C(\alpha - \alpha_c)]} \tag{8}$$

where k_c is the rate constant for chemical kinetics, k_e is the overall effective rate constant, C is a constant, and α_c is a critical value. The α_c value is thought as

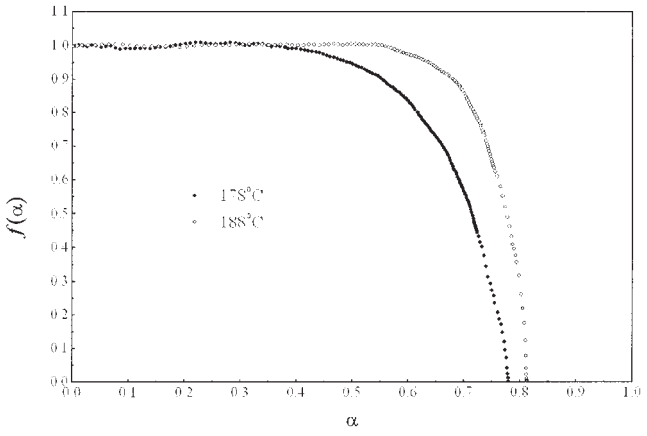

Figure 9 Plots of $f(\alpha)$ versus conversion for the Bis-ANER/DDS system at 178 and 188°C.

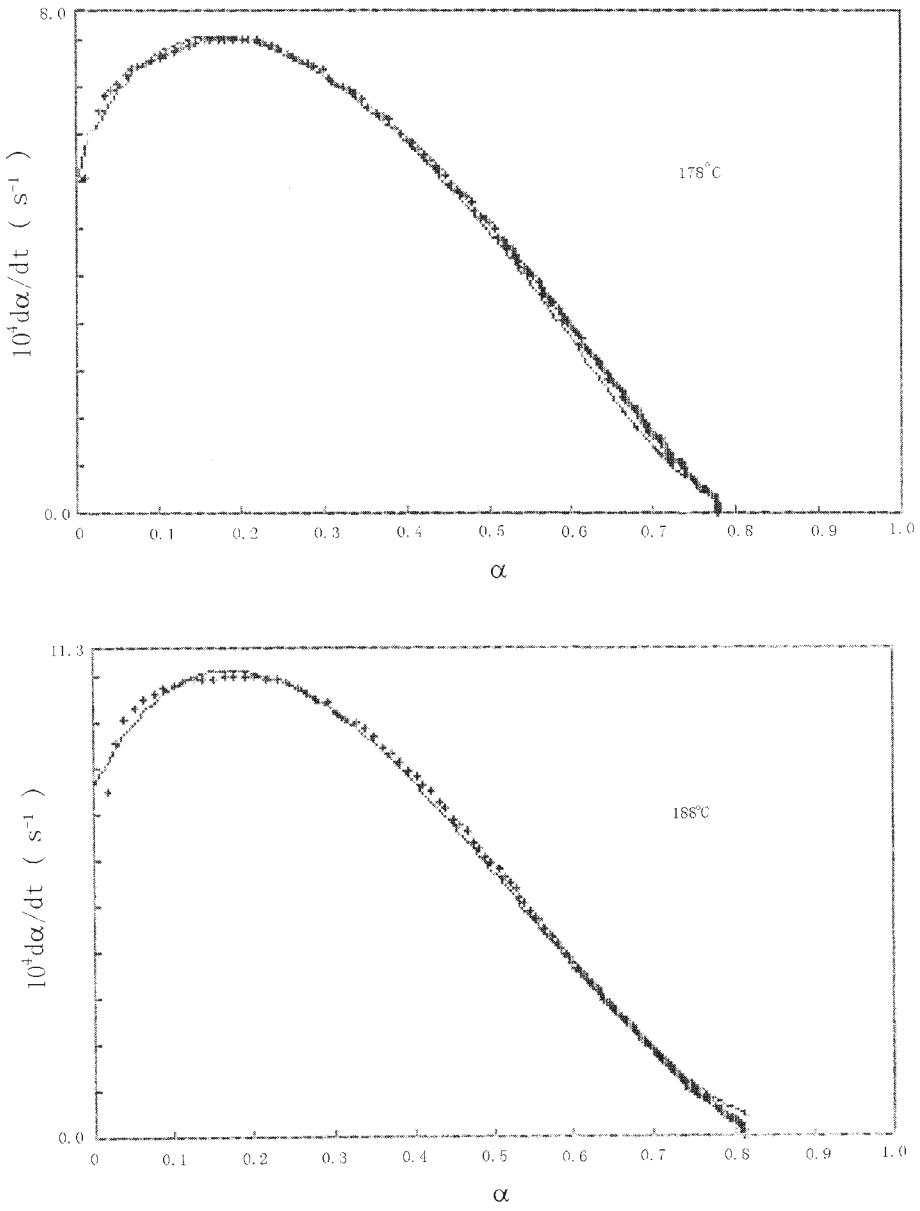

Figure 10 Comparison of (+) the experimental data with the (· · ·) kinetic model results with the $f(\alpha)$ for the Bis-ANER/DDS system at 178 and 188°C.

the onset of diffusion control, although the onset is somewhat more gradual, and there is a region where both chemical and diffusion control are significant.

The $f(\alpha)$ data were obtained by division of the experimental $d\alpha/dt$ values by those calculated from the autocatalytic model [eq. (6)]. The plots of $f(\alpha)$ versus α at 178 and 188°C are presented in Figure 9, and the comparison of the experimental data with the theoretical curves is shown in Figure 10. They matched well in the entire curing process. So the curing behavior at lower temperature could be described with the kinetics model with $f(\alpha)$.

CONCLUSIONS

Bis-ANER was synthesized via epoxidization of the Bis-ANR obtained from the reaction between BPA and formaldehyde. ^{1}H-NMR spectroscopy and GPC measurements indicated that Bis-ANR products consisted mainly of trimers plus some dimers. The curing process of Bis-ANER and DDS was studied with both dynamic and isothermal modes with DSC. The dynamic curing E values evaluated by the Kissinger and Flynn–Wall–Ozawa methods were 62.7 and 67.1 kJ/mol, respectively. The isothermal curing reaction followed the autocatalytic mechanism, and the curing

kinetics were described by the Kamal kinetics model, which accounted for both autocatalytic and diffusion-controlling effects. With increasing curing temperature, the fraction of autocatalytic effects increased and that of the diffusion effects decreased, which diminished at 208°C.

References

1. Imura, T.; Murata, Y.; Nakanishi, Y. U.S. Pat. 5,623,031 (1997).
2. Wang, C. S.; Lee, M. C. J Appl Polym Sci 1998, 70, 1907.
3. Kopf, P. W. Encyclopedia of Polymer Science and Engineering, 2nd ed.; Wiley: New York, 1988; Vol. 11.
4. Gardziella, A.; Pilato, L. A.; Knop, A. Phenolic Resins; Springer-Verlag: Berlin, 2000.
5. Kopf, P.; Wagner, E. J Polym Sci 1973, 11, 939.
6. Gipstein, E.; Ouano, A. C.; Tompkins, T. J Electrochem Soc 1982, 129, 201.
7. Gouri, C.; Reghunadhan Nair, C. P.; Ramaswamy, R. Polym Int 2001, 50, 403.
8. Ho, T. H.; Wang, C. S. J Appl Polym Sci 1999, 74, 1905.
9. Lin, C. H.; Chiang, J. C.; Wang, C. H. J Appl Polym Sci 2003, 88, 2607.
10. Kaji, M.; Nakahara, K.; Ogami, K.; Endo, T. J Polym Sci Part A: Polym Chem 1999, 37, 3687.
11. Kissinger, H. E. Anal Chem 1957, 29, 1702.
12. Flynn, J. H.; Wall, L. A. Polym Lett 1966, 4, 232.
13. Ozawa, T. Bull Chem Soc Jpn 1965, 38, 1881.
14. Kamal, M. R. Polym Eng Sci 1974, 14, 231.
15. Kamal, M. R.; Sourous, S. Polym Eng Sci 1973, 13, 59.
16. Dutta, A.; Ryan, M. E. J Appl Polym Sci 1979, 24, 635.
17. Ryan, M. E.; Dutta, A. Polymer 1979, 20, 203.
18. Khanna, V.; Chanda, M. J Appl Polym Sci 1993, 49, 319.
19. Barral, L.; Cano, J.; Lopez, A. J.; Lopez, J.; Nogueira, P.; Ramirez, C. J Appl Polym Sci 1995, 56, 1029.
20. Cook, W. D.; Simon, G. P.; Burchill, P. J.; Lau, M.; Fitch, T. J. J Appl Polym Sci 1997, 64, 769.
21. Cole, K. C.; Hechler, J. J.; Noel, D. Macromolecules 1991, 24, 3098.